ISSN 8755-6839

SCIENCE OF **TSUNAMI HAZARDS**

Journal of Tsunami Society International

Volume 30 **Number 3** **2011**

THE RESPONSE OF MONTEREY BAY TO THE GREAT TOHOKU EARTHQUAKE OF 2011

L. C. Breaker[1], T. S. Murty[2], D. Carroll[1] and W. J. Teague[3]

[1] Moss Landing Marine Laboratories, Moss Landing, CA 93950
[2] University of Ottawa, Ottawa, Canada
[3] Naval Research Laboratory, Stennis Space Center, MS 39529

ABSTRACT

The response of Monterey Bay to the Great Tohoku earthquake of 2011 is examined in this study. From a practical standpoint, although the resulting tsunami did not cause any damage to the open harbors at Monterey and Moss Landing, it caused extensive damage to boats and infrastructure in Santa Cruz Harbor, which is closed to surrounding waters. From a scientific standpoint, the observed and predicted amplitudes of the tsunami at 1 km from the source were 21.3 and 22.5 m based on the primary arrival from one DART bottom pressure recorder located 986 km ENE of the epicenter. The predicted and observed travel times for the tsunami to reach Monterey Bay agreed within 3%. The predicted and observed periods of the tsunami-generated wave before it entered the bay yielded periods that approached 2 hours. Once the tsunami entered Monterey Bay it was transformed into a seiche with a primary period of 36-37 minutes, corresponding to quarter-wave resonance within the bay. Finally, from a predictive standpoint, major tsunamis that enter the bay from the northwest, as in the present case, are the ones most likely to cause damage to Santa Cruz harbor.

Keywords: *Great Tohoku earthquake, Monterey Bay, damage reports, singular spectrum analysis, seiche modes*

1. INTRODUCTION

On March 11, 2011 at 05:46 UTC, one of the five largest earthquakes since 1900 hit the coast of Japan. It has been called The Great Tohoku Earthquake and had a magnitude (M_W) of 9.0, according to the Japanese Meteorological Agency (JMA) and the U.S. Geological Survey (USGS). It occurred 373 km northeast of Tokyo. The Pacific Tsunami Warning Center issued a tsunami warning for the entire Pacific Ocean within 2 hours after the earthquake occurred. Along the coasts of California and Oregon, tsunami-generated surges of up to 2.4 m hit some areas, causing major damage to docks and harbors. At Crescent City, California, the tsunami produced a wave height of 7 feet (2.1 m), a location where extensive damage occurred. A state of emergency was declared for several counties in California including Del Norte, Humboldt, San Mateo, and Santa Cruz.

Monterey Bay is directly exposed to the open ocean with an entrance that is almost as wide as the bay itself. It has three harbors, one at Monterey at the south end of the bay, a second at Moss Landing at the center of the bay, and a third at Santa Cruz at the north end of the bay (Fig. 1). Between 8:00AM and 9:00AM PDT, sudden increases in water level of almost a meter were reported at Monterey and Moss Landing. The Pacific Tsunami Warning Center (PTWC) reported a peak amplitude in water level of 70 cm at Monterey (B. Shiro, personal communication). No significant damage to infrastructure or boating was reported at either location. However, at Santa Cruz Harbor extensive damage did occur. Conservative estimates indicate that losses to infrastructure in Santa Cruz Harbor approach $30M and that up to 100 boats experienced significant damage resulting in losses that exceed $5M. Unlike Monterey and Moss Landing, the Santa Cruz Harbor is essentially closed and so was unable to accommodate the incoming waters associated with the tsunami leading to amplified surges and the resulting damage.

2. MATERIALS AND METHODS

a. Sources of Data

The data used in this report come from three sources. First, bottom pressure data were acquired from the Monterey Accelerated Research System (MARS) array (www.mbari.org/MARS/). The array is located beyond the entrance of Monterey Bay on a ridge near the edge of Monterey Submarine Canyon at a depth of 891m, approximately 25 km west-northwest of Monterey (Fig. 1). The pressure data from the MARS array was converted to equivalent sea surface height via the hydrostatic equation. Second, water levels at one-minute resolution were acquired from the tide gauge in Monterey Harbor. This tide gauge is part of NOAA's National Water Level Observation Network (NWLON) operated and maintained by the National Ocean Service. Finally, bathymetric data from the U.S. Navy with 2-minute resolution along a great circle path from the tsunami's point of origin to the MARS array was used to calculate expected travel times (Ko, 2009).

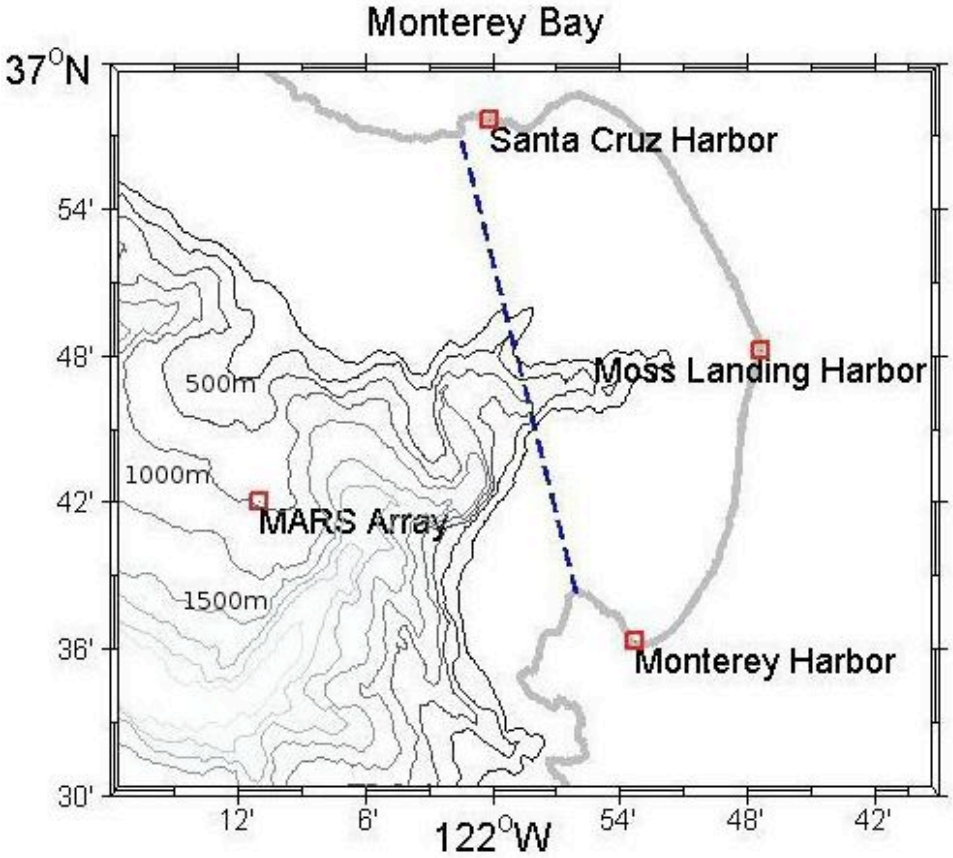

Fig. 1. This figure shows Monterey Bay together with the location of the MARS array where the pressure data were acquired, and the three harbors within the bay. The dashed line represents the expected nodal location for the transverse mode of oscillation for Monterey Bay.

b. Method of Analysis

To examine the response of Monterey Bay, Singular Spectrum Analysis (SSA) was employed (e.g., Breaker et al., 2011). SSA is a method of decomposing a time sequence into a set of independent modes, similar in many respects to Principal Component Analysis (PCA). Because of the adaptive nature of the basis functions employed the method is well-suited for analyzing records that are nonstationary and/or nonlinear (e.g., Vautard et al., 1992). SSA can be applied to short, noise-like time series, making it well-suited for use in this study.

A lagged covariance matrix is formed from the time sequence (a Toeplitz matrix in this case) that is decomposed into eigenvalues, eigenvectors and principal components. Reconstructed components can be calculated from the eigenvectors and principal components that represent partial time series whose sum over all modes reproduces the original time series. The number of modes that are selected is called the window length and determines the resolution of the decomposition. The results of the SSA analysis are presented in the following section.

3. RESULTS

a. Initial Conditions

The epicenter of the Great Tohoku Earthquake was located approximately 72 km east of the Oshika Peninsula of Tōhoku at a depth of 32 km. This event has been categorized as an undersea megathrust rupture that occurred along the Japan Trench subduction zone with the Pacific Plate subducting beneath the plate that underlies northern Honshu. The rupture caused the sea floor to rise by 5 - 8 meters. According to the JMA, the earthquake may have ruptured the fault zone over a length of 500 km and a width approaching 200 km. The JMA analysis also indicated that the earthquake itself was comprised of a set of three events. The co-seismic, vertical motion of the seafloor produced a devastating tsunami that was felt over the entire Pacific basin. Tectonically generated vertical subsidence likely intensified the tsunami. The Tohoku earthquake was followed by three aftershocks that exceeded 7.0 M_w within 45 minutes of the main event.

We have extracted the arrival sequences for the Great Tohoku Earthquake from three Deep-ocean Assessment and Reporting of Tsunamis (DART) bottom pressure recorders (www.ndbc.noaa.gov/dart/dart.shtml). DART bottom pressure recorders 21418, 21401, and 21413 were employed. The DART recorders are located in deep water away from coastal influences at distances of 551, 986, and 1224 km, East, ENE and SE of the epicenter. We have estimated the amplitude of the tsunami at 1 km from the source assuming cylindrical spreading and thus the effects of refraction have not been taken into account. The primary signals were distinct at 21413 and 21401 but not at 21418 and so we have not included the results from this location.

To obtain a first-guess value for the amplitude we have used the following empirical relation: $Log_{10}H = 0.75 \cdot M_w - 5.07$, where H is the amplitude in meters and M_w is the earthquake magnitude (Camfield, 1980). For M_w equal to 9.0, we obtain a value for H of 22.5 m. Amplitudes of 68.1 and 78 cm were estimated from the arrival sequences at the bottom pressure recorders yielding amplitudes at the source of 21.3 and 27.5 m for BPRs 21401 and 21413, respectively. Although a value of 21.3 m is relatively close to the predicted value, a value of 27.3 m appears high and could reflect phase interference in the primary signal, errors accrued because the effects of refraction were not taken into account, or that the empirical relation used to obtain the first-guess provides only a rough estimate of the true value.

b. Propagation of the Tsunami across the Pacific

To a first approximation, the tsunami generated by the Great Tohoku earthquake has been assumed to follow a great circle trajectory as shown in the upper panel of Fig. 2. To test the validity of this assumption we have compared the observed travel time between the epicenter and the MARS array, with that obtained by calculating $S/\sqrt{g\overline{H}}$, where S is the great circle distance, $\overline{H}$, the mean depth along the great circle path, g, the acceleration of gravity, and $\sqrt{g\overline{H}}$ represents the shallow-water phase speed for non-dispersive waves. The bathymetry along the great circle trajectory is shown as a depth profile in the lower panel of Fig. 2. The mean depth, $\overline{H}$, is 4825 m (horizontal red line).

The observed travel time was approximately 9 hours and 50 minutes, and the calculated travel time over a distance of 8012.3km was 10 hours and 7 minutes, or about 2.7% longer than the observed travel time. Similar comparisons in the past have shown that in some cases the observed travel times are shorter than the calculated travel times, and in others, the reverse. Finally, our calculated travel time is very close to the value obtained from the National Geophysical Data Center's travel time map for the tsunami, which does include the effects of refraction. Their analysis yielded a value of 10 hours and 4 minutes (www.ngdc.noaa.gov/hazard/honshu_11mar2011/).

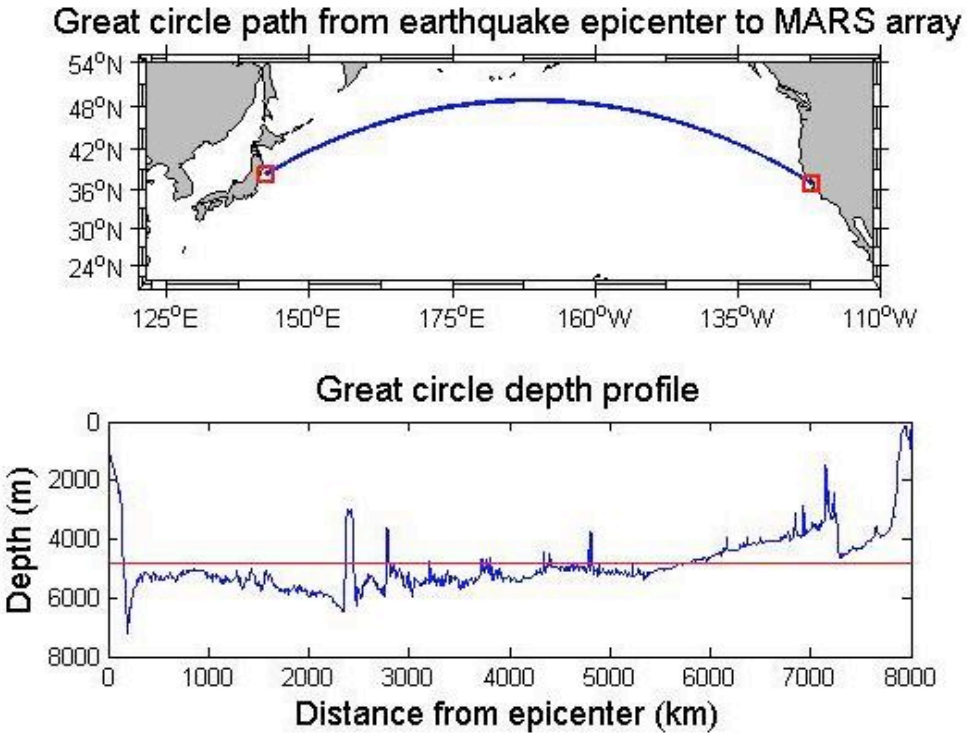

Fig. 2. The upper panel shows the great circle track from the earthquake epicenter to the MARS array located just beyond the entrance to Monterey Bay. The lower panel shows the depth profile along the great circle track. The horizontal red line corresponds to a mean depth of 4825m along the entire track.

c. The Tsunami Prior to Entering Monterey Bay

Fig. 3 (upper panel) shows the tsunami as observed at the MARS array before it entered Monterey Bay. We do not often have the opportunity to observe tsunamis in the absence of coastal influences because most tide gauges that record these events are located along the coast. The predicted period of the tsunami, T, can be approximated by $log_{10}\, T = 0.625 \cdot M_w - 3.31$, yielding a value of about 135 minutes (Wilson and Torum, 1968). As we look at the arrival sequence at least three well-defined peaks occur within this period, consistent with the JMA analysis. The first peak, and by far the largest, has an amplitude of approximately 25 cm. The largest aftershocks may have also generated secondary

tsunamis that contributed to the arrival sequence. Although only the first 12 hours of the arrival sequence are shown, it continued for at least five days before settling down to background levels. Because major peaks in the wave train occurred for many hours after the first arrival, the extended arrival sequence contains transoceanic reflections of the main event from many locations around the North Pacific basin (Murty, 1977). Overall, the reverberation times following such an event are expected to be on the order of a week (Munk, 1963).

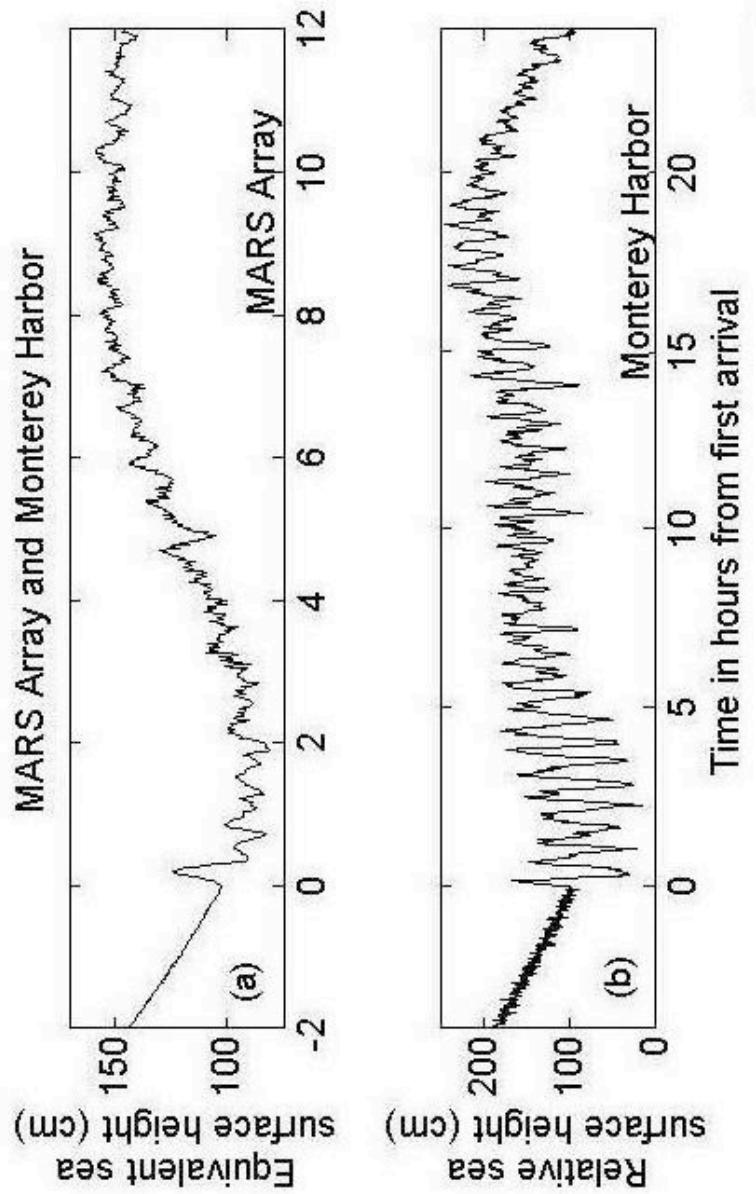

Fig. 3. The upper panel shows the pressure signal (converted to equivalent surface elevation) recorded at the MARS array for the tsunami generated by the Great Tohoku Earthquake starting two hours before the first arrival. The lower panel shows one-minute water levels recorded at the tide gauge in Monterey Harbor starting four hours before the first arrival.

On closer inspection, the trace also contains a 3-4 minute oscillation that is superimposed on the wave train starting about two hours into the arrival sequence. This oscillation may be due to interaction of the tsunami with the ridge upon which the pressure transducer is located. To explain in more detail, there are basically two different types of oceanic oscillations, oscillations of the First Class (OFC), also referred to as Gravoid modes that exist with or without the rotation of the earth, although their frequencies are modified due to earth rotation and gravity appears explicitly in their frequency equation (Murty and El-Sabh, 1986). These have periods of the order of a few minutes to several hours, depending upon the geometry of the water body and the bathymetric gradients. Oscillations of the Second Class (OSC), often called rotational modes (Elastoid-inertia modes), owe their existence to the rotation of the earth and gravity does not play a significant role in the frequencies they represent. OFC and OSC are separated in frequency by the so-called Pendulum day, which depends upon the latitude, with OFC having periods smaller then the Pendulum Day and OSC having periods greater than the Pendulum Day.

A similar situation occurred during the Indian Ocean tsunami of December 26, 2004 where oscillations of both OFC and OSC types were identified in sea level observations along the coastlines of India (Nirupama et al., 2005a; Nirupama et al., 2005b). In the present case, however, it appears that the 3-4 minute period oscillations are of the OFC type because of their relatively short period, i.e., less than a Pendulum day, and arose when the tsunami wave encountered the steep bathymetric gradients leading up to the MARS array. Such gradients that occur on coastal shelves, shelves around islands, seamounts, ridges and valleys, have been shown to generate short-period waves of the types described above during other tsunamis as well (e.g., Neetu et al., 2011).

d. The Tsunami Transformation after Entering the Bay

Once the tsunami entered Monterey Bay, it was transformed into a series of resonant oscillations often called seiche modes. This process is well-known and has been studied in some detail in Monterey Bay (e.g., Breaker et al., 2010). The lower trace in Fig. 3 (lower panel) shows the broadband response based on one-minute sampling of water levels from the tide gauge in Monterey Harbor (Fig. 1). According to our observations, the amplitude of the first arrival in the sequence has an amplitude of approximately 75cm, close to the value reported by the Pacific Tsunami Warning Center (70cm). Amplitudes inside the bay far exceed the amplitude of the tsunami outside the bay due to the excitation of resonant modes of oscillation whose periods are dictated by the boundaries that constrain them.

Returning to Singular Spectrum Analysis (SSA) as described in Section 2, the method was used to decompose the tidal record from Monterey. First, SSA was used to remove the diurnal and semidiurnal tides with a window length of 1000 minutes. The residuals were then subjected to a second SSA using a window length of 160 minutes. The reconstructed modes corresponding to the five largest eigenvalues are shown in Fig. 4. The modes are shown in order of decreasing period from top to bottom. The primary mode of oscillation is shown in the second panel. This highly resonant mode, as indicated by the purity and regularity of the waveform, has a period of 36-37 minutes, and corresponds to the transverse mode of oscillation that assumes a nodal line across the entrance of the

bay (Fig. 1). This oscillation corresponds to quarter-wave resonance and was observed previously for the Great Alaskan Earthquake of 1964 (Breaker et al., 2009). Both tsunamis entered the bay from the northwest. This mode also reveals a modulation period of slightly over 12 hours and so may reflect the influence of the semidiurnal tide.

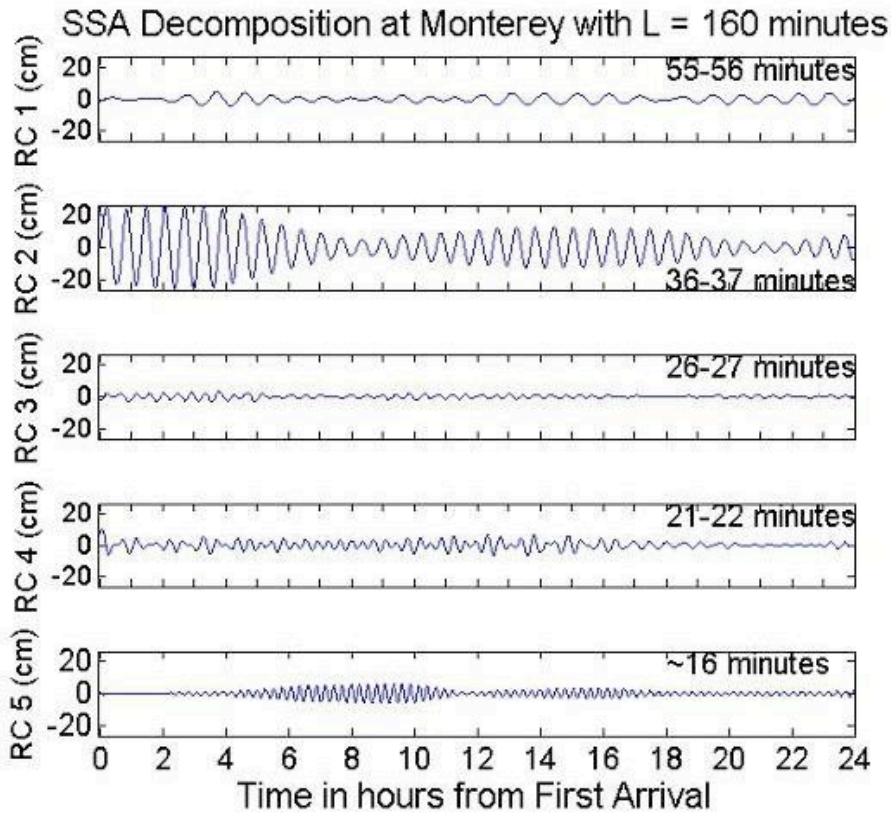

Fig. 4. This figure shows a Singular Spectrum Analysis (SSA) decomposition of the one-minute water level data from the tide gauge into a sequence of five independent modes for the first 24 hours following the first arrival. The label, "RC", on the vertical axis refers to "Reconstructed Component".

The top panel shows an oscillation with a period of 55-56 minutes and corresponds to the longitudinal mode for Monterey Bay and has been observed on numerous occasions. We note that there was a delay of almost two hours before this mode was fully excited. The third panel shows a weak response for the mode with a period of 26-27 minutes, a mode that has likewise been observed in the past. The fourth panel shows a frequently observed mode with a period of 21-22 minutes. Finally, the fifth panel shows a highly resonant oscillation with a period of approximately 16 minutes, a mode that was not fully excited until several hours into the sequence.

Previous studies have shown that all of the modes except for the longitudinal mode (top panel) have higher amplitudes in the southern part of the bay near Monterey and at the north end of the bay near Santa Cruz. Higher amplitudes at the north end of the bay undoubtedly contributed to the extensive damage that occurred in Santa Cruz Harbor.

4. SUMMARY AND CONCLUSIONS

The tsunami-generated wave before it entered Monterey Bay contained an oscillation with a period of 3-4 minutes that was most likely generated by interaction of the incoming wave as it approached the ridge where the MARS array is located, and the local bathymetry. The response of Monterey Bay to the tsunami in terms of its resonant behavior was primarily characterized by quarter-wave resonance with a period of 36-37 minutes, corresponding to the bay's transverse mode of oscillation. Although other modes of oscillation were excited their responses were overshadowed by the primary response.

The response to the tsunami generated by the Great Tohoku Earthquake in terms of the damage incurred inside the bay was extensive but confined to Santa Cruz Harbor. For the purpose of issuing warnings, for tsunamis that enter the bay from the northwest which will be the case for most earthquakes that are generated along the Pacific Rim from Japan to the Gulf of Alaska and down the west coast of North America, it is likely that Santa Cruz Harbor could again experience significant damage for events whose magnitudes approach those of the Great Tohoku and Great Alaskan earthquakes.

5. ACKNOWLEDGMENTS

We thank Cary Wong from NOAA's National Ocean Service for providing the one-minute water level data from Monterey, and William Chadwick for providing the bottom pressure data from the MARS array through the courtesy of Oregon State University and NOAA/PMEL, with funding from National Science Foundation grant OCE-0826490. We also thank Paula Dunbar from the National Geophysical Data Center for the travel time estimate presented in section 4. Finally, we gratefully acknowledge eyewitness accounts of the wave impacts on Monterey, Moss Landing and Santa Cruz Harbors from Steve Scheiblauer, Lee Bradford, and Dan Haifley.

6. REFERENCES

Breaker, L.C., Y.-H Tseng, and X. Wang (2010), On the natural oscillations of Monterey Bay: Observations, modeling, and origins. Progress in Oceanography, 86, 380-395.

Breaker, L.C., T.S. Murty, J.G. Norton, and D. Carroll (2009), Comparing the sea level response at Monterey, California from the 1989 Loma Prieta earthquake and the 1964 Great Alaskan Earthquake. Science of Tsunami Hazards, 28, 255-271.

Camfield, F.E. (1980), Tsunami Engineering. Special Report No. 6, U.S. Army Corps of Engineers, Coastal Engineering Research Center, Fort Belvoir, VA, 222 pp.

Ko, D.S. (2009), DBDB2 v3.0 Global 2-minute Topography. http://1117320.nrlssc.navy.mil/DBDB3_WWW. Naval Research Laboratory, Oceanography Division, Ocean Dynamics and Prediction Branch.

Munk,W.H. (1963), Some comments regarding diffusion and absorption of tsunamis. In: D.C. Cox (ed.). Proc. tsunami meetings associated 10th Pac. Sci. Congr. , Honolulu, Hawai. Union Geod. Geophys. Monogr. 24. pp. 53-72.

Murty, T.S. (1977), Seismic Sea Waves – Tsunamis. Bulletin 198, Department of Fisheries and the Environment Fisheries and Marine Service. D.W. Friesen & Sons, Ltd, Altona, Manitoba, Canada.

Murty, T.S. and M.I. El-Sabh (1986), Gravitational oscillations in a rotating paraboloidal basin: a classical problem revisited. Mahasagar (Bull. Of the National Inst. of Oceanography, Goa, India), 18(2), 99-127.

Neetu, S., I. Suresh, R. Shankar, B. Nagarajan, R. Sharma, S.S.C. Shenoi, A.S. Unnikrishnan, and D. Sundar (2011), Trapped waves of the 27 November 1945 Makran tsunami: observations and numerical modeling. Natural Hazards, DOI 10.1007/s11069-011-9854-0.

Nirupama, N., T.S. Murty, A.D. Rao and I. Nistor (2005a), The Role of Gravoid and Elastoid Modes in oscillations around Andaman and Nicobar Islands. In Indian Ocean Tsunami, Ed: V. Sundar, Indian Institute of Technology Madras, India, 41-52.

Nirupama, N., T.S. Murty, A.D. Rao and I. Nistor (2005b), Tsunami in Andaman and Nicobar Islands: Oscillations of the First and Second Class. In Indian Ocean Tsunami, Ed: V. Sundar, Indian Institute of Technology Madras, India, p. 22-30.

Vautard, R., P.Yiou, and M. Ghil (1992), Singular spectrum analysis: A toolkit for short, noisy chaotic signals. Physica D, 58, 95-126.

Wilson, B.W., and A. Torum (1968), The tsunami of the Alaskan earthquake, 1964: Engineering evaluation. U.S. Army Corps. Eng. Coastal Eng. Res. Cent. Tech. Memo 25, 401 pages.